KeAi

CHINESE ROOTS
GLOBAL IMPACT

Contents lists available at ScienceDirect

Petroleum Science

journal homepage: www.keaipublishing.com/en/journals/petroleum-science



Original Paper

Study on swelling and retention of liquid hydrocarbon compounds by type I kerogen



Tian Liang ^{a,b,*}, Yan-Rong Zou ^{a,b}, Zha-Wen Zhan ^{a,b}, Ping-An Peng ^{a,b}

- ^a State Key Laboratory of Deep Earth Processes and Resources, Guangzhou Institute of Geochemistry, Guangzhou, 510640, Guangdong, China
- ^b University of Chinese Academy of Sciences, Beijing, 100049, China

ARTICLE INFO

Article history: Received 20 June 2024 Received in revised form 13 June 2025 Accepted 20 July 2025 Available online 25 July 2025

Edited by Xi Zhang and Jie Hao

Keywords: Swelling Type I kerogen Shale oil Expulsion

ABSTRACT

In this paper, experiments were carried out to investigate the retention of liquid hydrocarbons in kerogen type I. The study focuses on the mudstone from the Lucaogou Formation in the Junggar Basin of China. To prepare samples of kerogen with varying degrees of maturity, artificial pyrolysis was used. Swelling experiments with three different types of liquid hydrocarbons were then conducted. The results revealed that the peak swelling adsorption capacity of type I kerogen for liquid hydrocarbons occurred at Easy $R_0 = 1.07$. Additionally, the kerogen showed a selective ability to retain aromatic hydrocarbons throughout the entire process compared to alkane. The order of hydrocarbon expulsion from source rocks was established as follows: short-chain alkanes > cycloalkanes/long-chain alkanes > aromatics with alkyl groups > polycyclic aromatic hydrocarbons. This study also developed a model for evaluating the swelling capacity of kerogen. This model was capable of evaluating the total swelling state of liquid hydrocarbons without considering the adsorption state, which was not possible in previous experimental work. According to this model, the swelling ability of long-chain alkanes and polycyclic aromatic hydrocarbons in type I kerogen was high, while the swelling ability of cycloalkanes was weak, and most of them existed in the form of adsorption. This study suggests that paraffin and asphaltenes may affect the expulsion of shale oil and heavy oil in the form of swelling state, particularly in immature source rocks. This finding provides a new direction for research on hydrocarbon source rock evaluation and unconventional oil exploration.

© 2025 The Authors. Publishing services by Elsevier B.V. on behalf of KeAi Communications Co. Ltd. This is an open access article under the CC BY-NC-ND license (http://creativecommons.org/licenses/by-nc-nd/4.0/).

1. Introduction

Kerogen is a substantial molecule organic substance commonly discovered in sedimentary rocks and serves as a significant source of organic carbon in the crust (Berger, 1960; Hunt, 1972; Durand and Monin, 1980). Kerogen can be divided into three types, I, II, and III, based on the parent material and composition. Type I kerogen, also known as sapropelic kerogen, is derived from lacustrine algae mainly. It has a high H/C ratio (usually greater than 1.5) and the O/C ratio varies between 0.03 and 0.1 (Fester and Robinson, 1966; Mao et al., 2010; Vandenbroucke and Largeau,

Based on the chemical structure and source of type I kerogen, it exhibits the highest potential for hydrocarbon generation in comparison to the other two types (Klemme and Ulmishek, 1991;

E-mail address: liangtian@gig.ac.cn (T. Liang).

Peer review under the responsibility of China University of Petroleum (Beijing).

^{2007).} The chemical structure of type I kerogen comprises a substantial number of aliphatic chains and a minimal number of aromatic ring structures, making it simple to break down into hydrocarbons during pyrolysis. In contrast, type II and III kerogen possess lower H/C and higher O/C values, as well as a higher proportion of aromatic carbon. Tissot et al. (1978) conducted the first study on type I kerogen in the Unita Basin of the United States, and subsequent researchers found that type I kerogen is widespread in sedimentary basins around the world, including the Autun black shale in Massif Central, France; the torbanite in the Blue Mountains of the Sydney Basin, Australia; the Late Cretaceous Yacoraite in the Salta Basin, Argentina and the kerogen of the Lucaogou Formation in the Junggar Basin, Xinjiang Province, China (Berlendis et al., 2014; Romero-Sarmiento et al., 2019; Zhang and Volkman, 2020; Liang et al., 2023).

^{*} Corresponding author.

T. Liang, Y.-R. Zou, Z.-W. Zhan et al. Petroleum Science 22 (2025) 3960–3966

Vandenbroucke and Largeau, 2007). According to Cao et al. (2021), the hydrocarbon yield of type I kerogen from the Qingshankou Formation in the Songliao Basin, NE China reached over 70% during its peak stage ($R_0 = 0.89\%-1.34\%$). Lewan and Roy (2011) and Behar et al. (2010) demonstrated that significant amounts of hydrocarbons can be produced through the pyrolysis of Green River kerogen, whether there is water or not. However, current technology can only extract hydrocarbons in free and pore states from source rocks, and cannot obtain swollen and adsorbed state hydrocarbons from kerogen and source rock (van Heek, 2000; Jarvie, 2012; Larter et al., 2012; Hu et al., 2021). The ability of kerogen to swell and adsorb hydrocarbons has raised concerns among researchers about evaluating the total amount of swollen hydrocarbons (Li et al., 2016; Wei et al., 2012).

In recent years, swelling experiments have been utilized to assess the amount of liquid organic matter retained in kerogen, with most studies employing solubility parameters to conduct this test (Sandvik et al., 1992; Kelemen et al., 2006; Kilk et al., 2010; Huang et al., 2020; Liang et al., 2021). Li et al. (2016) employed this method to quantify the relative oil retention capacities of clay minerals, quartz, and carbonate in oil shale from the Dongying Depression in the Bohai Bay Basin, reporting values of 18.0, 3.0, and 1.8 mg/g, respectively. This study further identified the optimal depths for shale oil exploration as ranging between 3400 and 3600 m (Li et al., 2016). In a separate investigation, Wei et al. (2012) examined the retention of saturated hydrocarbons, aromatics, resins, and asphaltenes in source rocks obtained from the Niuzhuang Sag in the Bohai Bay Basin, Liang et al. (2025) found that when the centrifugal force exceeded 647.4 g. only liquid organic matter in swollen and adsorbed states remained in kerogen. However, using solubility parameters as the criterion has led to a lack of systematic evaluation of the adsorption of series hydrocarbons by kerogen, including saturated and aromatic hydrocarbons, and the mechanism of this process has not been fully understood. On the other hand, the semi-quantitative distinction between swollen and adsorbed liquid hydrocarbons in kerogen is still not fully realized (Liang et al., 2025). Ballice (2003) highlighted the presence of anomalies in the swelling process of some liquid organic compounds, such as ethanol, which may cause discrepancies in the quantitative results of related studies that use these compounds as solubility parameters.

Therefore, this study focused on type I kerogen and prepared kerogen samples with different maturities through artificial pyrolysis simulation experiments. Common hydrocarbon compounds found in petroleum were selected as the liquid organic matter for conducting swelling experiments. The objective of this research was to investigate the influence of kerogen evolution degree on the swelling and adsorption amount of hydrocarbons, explore the competitive swelling and adsorption of different hydrocarbons in kerogen, and analyze the mechanism underlying this process. To achieve these goals, the study established an evaluation model for the swelling amount of liquid organic matter after removing the adsorption part and systematically analyzed the interaction process between type I kerogen and hydrocarbons.

2. Samples and methods

2.1. Samples

The rock sample was collected from the Lucaogou Formation located in the Dalongkou area of Jimusaer Sag in Junggar Basin, Xinjiang province, China. The source rocks of the Lucaogou Formation (LCG) are arranged in an anticline pattern. The oil shale of this formation is the primary source rock in the Junggar petroliferous basin and is a semi-deep to deep lacustrine deposit within

the basin. According to the results of Rock-eval, the Lucaogou kerogen has a high potential of hydrocarbon generation (HI is 704 and S2 is 464.82 mg/g TOC) and belongs to type I (Table 1). Table 2 showed the results of elemental analysis of kerogen, with the increase of maturity, the relative proportion of hydrogen decreased continuously, and the H/C atomic ratio showed the same trend. This indicates that the increase of maturity causes the continuous cracking of the original kerogen samples.

The rock sample was ground to 120 mesh and extracted with the solvent mixture composed of dichloromethane and methanol (93:7 v:v) to remove the soluble organic matter. Then, the hydrochloric acid (6 mol/L) and hydrofluoric acid (6–8 mol/L) were added sequentially to decompose the inorganic minerals. The sample was rinsed repeatedly with deionized water until the pH reached 7. Finally, the sample was extracted with a solvent mixture of dichloromethane and methanol (93:7 v:v) again to remove the soluble organic matters adsorbed by minerals, and a pure kerogen sample was obtained (GB/T19144-2010).

2.2. Artificial pyrolysis

The initial kerogen powder was loaded into gold tubes which were sealed at both ends after replacing the air inside with argon. Each tube was subsequently placed in a separate autoclave, and these autoclaves were placed in a common furnace. The pressure inside the autoclaves was set to 50 MPa, and the temperature in the furnace was elevated in three stages; first, the temperature was increased from room temperature to 300 °C in 8 h; second, the temperature was maintained at 300 °C for 2 h; and third, the temperature was increased to 480 °C at a rate of 20 °C/h. During the whole experiment process, different temperature points corresponded to a defined maturity value of kerogen residues, which were evaluated using Easy%R₀ (Sweeney and Burnham, 1990; He et al., 2018, 2019). As the autoclaves were removed from the furnace at different temperature points (Easy R_0), each gold tube in the autoclaves represented a specific maturity level of the kerogen. The autoclaves were cooled, the pressure was released, and each gold tube was removed. Thereafter, the products were collected and separated (gas, light hydrocarbons, soluble organic matter, and kerogen residue). There were total nine kerogen residues with different maturity collected at corresponding temperature point: 360 °C (Easy% $R_{\rm o}=0.68$), 380 °C (Easy% $R_{\rm o}=0.77$), 390 °C (Easy% $R_0 = 0.83$), 400 °C (Easy% $R_0 = 0.89$), 410 °C (Easy% $R_0 = 0.98$), 420 °C (Easy% $R_0 = 1.07$), 440 °C (Easy% $R_0 = 1.28$), 460 °C (Easy% $R_0 = 1.52$), and 480 °C (Easy% $R_0 = 1.80$).

Table 1Basic geochemistry parameters of kerogen.

Sample	S _{1,} mg/g	S ₂ , mg/g	S ₃ , mg/g	T _{max} , °C	HI	Easy%R _o a	Туре
LCG	4.57	464.82	14.11	441	704	0.78	I

^a Easy% $R_o = T_{max} \times 0.018-7.16$ (Sweeney and Burnham, 1990).

Table 2 Results of elemental analysis.

Sample (Easy%R _o)	N, %	C, %	Н, %	S, %	H/C
L1 (0.68)	2.91	77.64	7.13	2.29	1.10
L2 (0.77)	2.96	77.70	6.22	1.60	0.96
L3 (0.83)	3.02	76.91	5.69	1.68	0.89
L4 (0.89)	3.67	75.31	4.73	2.19	0.75
L5 (0.98)	3.71	75.71	4.12	2.51	0.65
L6 (1.07)	3.60	76.62	3.93	2.09	0.62
L7 (1.28)	3.63	77.30	3.70	1.95	0.57
L8 (1.52)	3.73	78.56	3.49	2.20	0.53
L9 (1.80)	4.03	81.04	3.57	3.35	0.53

T. Liang, Y.-R. Zou, Z.-W. Zhan et al. Petroleum Science 22 (2025) 3960–3966

2.3. Swelling experiment

The swelling experiment was carried out by classical centrifugation (Wei et al., 2012; Li et al., 2016; Liang et al., 2025). As shown in Fig. 1, nine kerogen samples of varying maturities obtained through artificial pyrolysis were ground into powder and placed in a quartz tube with a small hole at the bottom, with the mass of the kerogen recorded as M_{ν} . The bottom of the quartz tube was blocked with quartz wool to ensure normal liquid flow, and the top was filled with quartz wool to prevent kerogen scattering during the experiment. The total weight of the quartz tube was M_1 . The quartz tube was then immersed in liquid organic matter for 72 h to ensure full contact between the kerogen and the liquid, promoting swelling. The liquid organic matters selected in this research, including *n*-hexane, *n*-octane, *n*-undecane, *n*-hexadecane, cyclopentane, cyclohexane, *n*-heptylbenzene, methylnaphthalene, and toluene, represented satureted, cycloalkanes, and aromatic hydrocarbon compounds commonly found in petroleum. After soaking, the quartz tube was wrapped in absorbent cotton and placed in a centrifuge, where the liquid organic matter was discharged at a speed of 3000 r/min, and the weight M_2 of the quartz tube was recorded. The amount of liquid organic matter adsorbed by unit mass of kerogen swelling was calculated as $(M_1-M_2)/M_k$, allowing for the evaluation of swelling capacity.

3. Results and discussions

The results of the swelling experiment for nine hydrocarbon liquid organic matter by kerogen samples with different maturities are presented in Table 3.

3.1. Swelling and adsorption of alkane

As shown in Fig. 2, the swelling adsorption capacity of kerogen for saturated hydrocarbons have no obviously changes before Easy $\Re R_0 = 0.89$, with all values being less than 0.25 g/g kerogen. However, as the maturity increases beyond 0.89, the swelling adsorption capacity increases significantly and is positively correlated with the chain length of saturated hydrocarbons. This

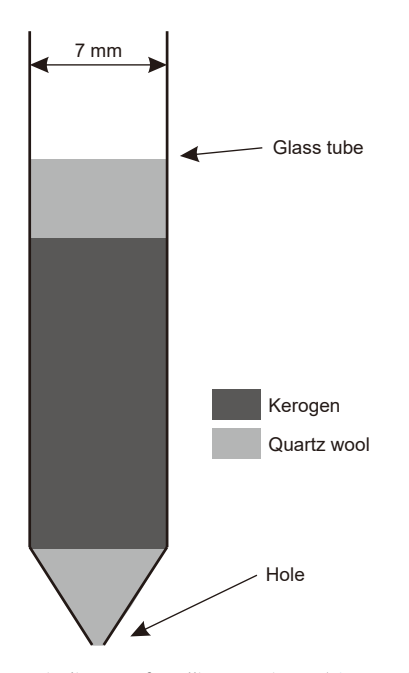


Fig. 1. Schematic diagram of swelling experiment (Liang et al., 2025).

suggests that kerogen is more likely to retain long-chain saturated hydrocarbons and expel short-chain saturated hydrocarbons as the maturity increases. The peak ability of kerogen to retain saturated hydrocarbons occurs around maturity of 1.07 during the entire thermal evolution.

The results of cyclopentane and cyclohexane are shown in Fig. 3. The swelling adsorption amount of cyclohexane in kerogen is more than that of cyclopentane throughout the artificial pyrolysis process. This indicates that kerogen molecules have a stronger ability to retain cycloalkanes compounds with more carbon atoms (Liang et al., 2023). When the carbon number is the same, the swelling adsorption capacity of cyclohexane is greater than that of *n*-hexane. Therefore, the swelling adsorption capacity of kerogen for liquid alkane compounds is: multi-carbon number cycloalkane > long-chain saturated hydrocarbon/low-carbon number cycloalkane > short-chain saturated hydrocarbon. Short-chain saturated hydrocarbon compounds are most easily expelled from the source rock.

3.2. Swelling and adsorption of aromatic hydrocarbon

The swelling adsorption results for *n*-heptylbenzene, methylnaphthalene, and toluene are depicted in Fig. 4. It is notable that methylnaphthalene exhibits a higher amount than n-heptylbenzene and toluene in nine kerogen samples. The molecular structure of methylnaphthalene contains more aromatic rings and hydrogen atoms than toluene, enabling it to form more π bonds and hydrogen bonds with aromatic ring clusters and electronegative atoms like oxygen or nitrogen in kerogen. In contrast, nheptylbenzene has a greater number of hydrogen atoms and fewer aromatic rings, resulting in the formation of more hydrogen bonds but fewer π bonds with kerogen molecules. These findings suggest that the interaction force between π bonds is stronger than that of hydrogen bonds during the interaction between liquid organic matter and kerogen. This phenomenon is further proved by the results of *n*-heptylbenzene and toluene. The molecular structure of *n*-heptylbenzene and toluene consists of only one aromatic ring, but *n*-heptylbenzene has twice as many hydrogen atoms as methylnaphthalene. However, in Fig. 4, the swelling adsorption of *n*-heptylbenzene and toluene is roughly equal, confirming that the π bonds are the primary energy in the interaction between aromatic compounds and kerogen, while hydrogen bonds are less significant.

3.3. Relationship between swelling adsorption and maturity of kerogen

The capacity of kerogen to swell and absorb liquid hydrocarbons is clearly divided into three stages with increasing maturity, as shown in Fig. 5 and Table 4.

In the first stage (Easy% $R_0 = 0.68-0.89$), the adsorption capacity is low and shows no significant changes (Table 3). Taking n-hexane as an example, the swelling adsorption capacity at this stage is 0.17, 0.17, and 0.18 g/g kerogen, respectively. This stage corresponds to the weak cracking of type I kerogen in the low maturity range, as noted by Gao et al. (2017). When the maturity is below 0.90, the hydrocarbon yield of LCG kerogen is less than 10%, in addition, a large amount of organic carbon is converted into asphaltenes (Table 4). Therefore, during this stage, the chemical structure of kerogen remains largely unchanged, resulting in no significant changes in swelling adsorption capacity.

In the second stage (Easy% $R_0 = 0.89-1.07$), the retention amount of saturated hydrocarbons, naphthenes, and aromatic hydrocarbons increases significantly, and the swelling adsorption capacity of kerogen to liquid hydrocarbons rises rapidly, reaching

Table 3Results of swelling experiment and density of each solvent.

Sample (%R _o)	n-hexane, g/g	n-octane, g/g	n-undecane, g/g	n-hexadecane, g/g	Cyclopentane, g/g	Cyclohexane, g/g	<i>n</i> -heptylbenzene, g/g	Methylnaphthalene, g/g	Toluene, g/g
L1 (0.68)	0.17	0.25	0.16	0.19	0.27	0.35	0.45	0.75	0.54
L2 (0.77)	0.17	0.20	0.13	0.17	0.24	0.27	0.61	0.65	0.49
L3 (0.83)	0.18	0.24	0.22	0.24	0.22	0.32	0.48	0.70	0.57
L4 (0.89)	0.53	0.54	0.59	0.67	0.36	0.68	0.81	1.45	0.95
L5 (0.98)	0.75	0.91	0.95	1.11	0.63	1.15	1.43	1.96	1.26
L6 (1.07)	1.02	0.96	1.04	1.36	0.84	1.36	1.59	2.06	1.41
L7 (1.28)	0.83	0.99	1.00	1.30	0.76	1.19	1.51	1.97	1.44
L8 (1.52)	0.71	0.87	0.98	1.28	0.56	1.11	1.34	1.88	1.23
L9 (1.80)	0.61	0.78	0.86	1.20	0.52	0.95	1.11	1.57	1.13

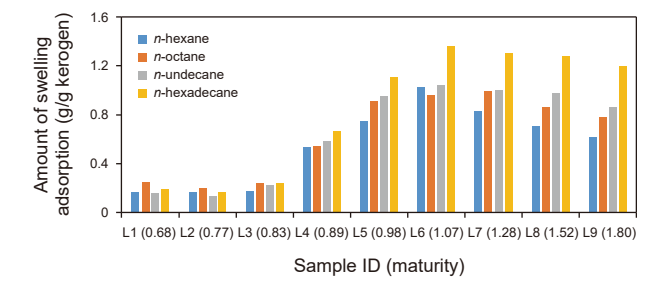


Fig. 2. Results of swelling experiment of saturated hydrocarbon.

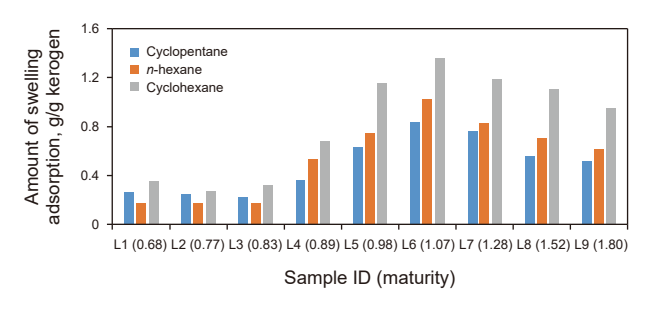


Fig. 3. Results of swelling experiment of cycloalkane hydrocarbon.

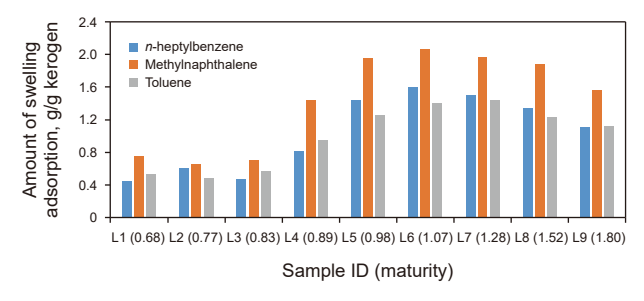


Fig. 4. Results of swelling experiment of aromatic hydrocarbon.

its peak. Taking n-hexane as an example, the swelling adsorption amount at this stage reaches a peak value of 1.02 g/g kerogen. As noted by Gao et al. (2017), after the maturity of 0.90, the ability of hydrocarbon generation of LCG kerogen increases significantly with the first structural jump occurring (Table 4). The pyrolysis of aliphatic chains and small aromatic rings in kerogen leads to an increase in organic pores, which can effectively swell and adsorb hydrocarbon compounds. This results in a rapid increase of the swelling adsorption capacity of the three types of liquid hydrocarbon.

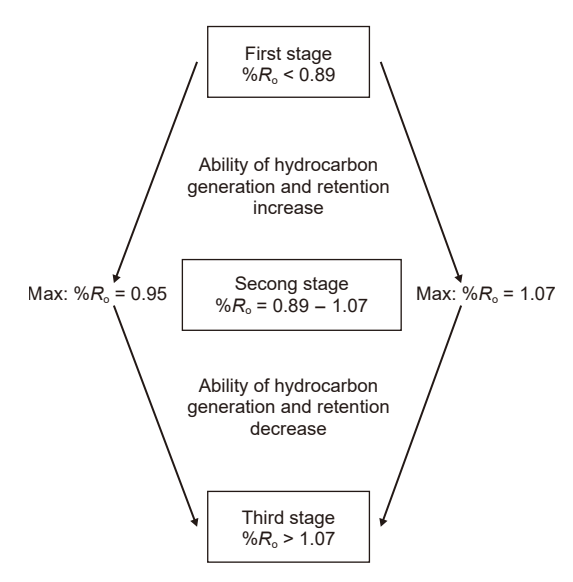


Fig. 5. Division of hydrocarbon expulsion stages of kerogen varying with maturity.

In the third stage (Easy $\Re R_0 > 1.07$), the swelling adsorption capacity of kerogen to liquid hydrocarbons decreases continuously. Taking n-hexane as an example, the amount of swelling dropped from the peak of 1.02 to 0.61 g/g kerogen during this period. Kerogen has passed the peak of hydrocarbon generation, and although the organic pores in kerogen structure are larger, but the aliphatic carbon has greatly reduced (Table 4). As noted by Liang et al. (2020), liquid hydrocarbon compounds mainly occur in the aliphatic carbon structure of kerogen. This leads to a continuous decrease in the adsorption ability of kerogen to liquid hydrocarbons in this stage.

The division of stages demonstrates that the swelling absorption capacity of type I kerogen for liquid hydrocarbons significantly increases after reaching a maturity level of 0.90 (Easy R_0), with a maximum at 1.07 (Easy R_0). Thereafter, the retention gradually decreases with increasing maturity.

Fig. 6 depicts the swelling adsorption proportion of saturated, naphthenic, and aromatic hydrocarbons in type I kerogen. The amount of each hydrocarbon is the average value of the same compound type in this study. As maturity increases, the proportion of saturated hydrocarbons increases from 17.70% to 30.17%, while the ratio of aromatic hydrocarbons decreases from 53.51% to 44.29%. Throughout the thermal evolution process, the proportion of cycloalkane remains relatively stable. This suggests that type I kerogen has the strongest capacity for retaining aromatic hydrocarbons. In the field of hydrocarbon expulsion, this phenomenon indicates that at the early stage of low maturity, a significant

Table 4Composition of pyrolysis products from Lucaogou Formation.

Sample	Easy%R _o	Hydrocarbon, mg	Resin + asphaltene, mg	Residual kerogen, mg
M9K-1	0.6	33.9	160.4	976.5
M9K-2	0.7	81.7	327.4	693.7
M9K-3	0.8	144.2	456.7	462
M9K-5	0.9	247.7	576.7	176.3
M9K-6	0.95	281.65	589.2	77.2
M9K-7	1	310.1	535.9	151.1
M9K-8	1.05	338.65	364.1	302.5
M9K-9	1.1	368.6	329.9	319.3
M9K-10	1.15	389.35	334.1	297.1
M9K-11	1.2	413.8	248.8	368
M9K-12	1.25	467.05	202	363.4
M9K-13	1.3	461.6	181.3	387.5
M9K-14	1.4	450.4	97	508.6
M9K-15	1.5	475.6	98.2	488.7
M9K-16	1.6	493.1	114.8	438.2

All of parameters are from Gao et al. (2017).

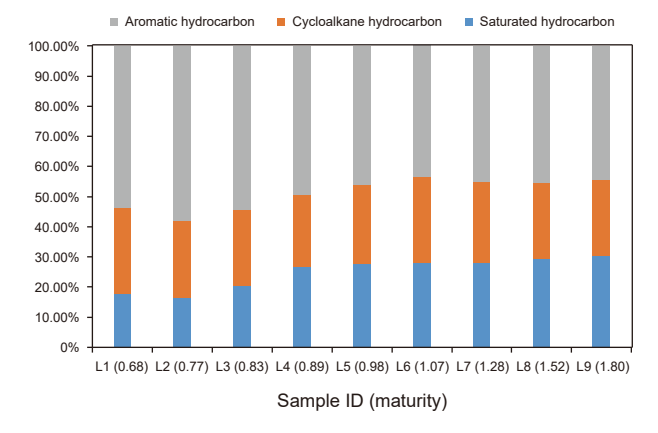


Fig. 6. Percentage of swelling capacity of different hydrocarbon compounds.

amount of saturated hydrocarbons are expelled from the source rock. As maturity increases, the expulsion of aromatic hydrocarbons also increases. The products of the entire process of hydrocarbon expulsion gradually transform from saturated to aromatic hydrocarbons.

3.4. Model for evaluating the swelling capacity of hydrocarbon in kerogen

Determining whether hydrocarbons in kerogen are in a swollen or adsorbed state has been a long-standing challenge in petroleum geochemistry research. Both states are often referred to as swelling adsorption for quantitative evaluation (Wei et al., 2012; Li et al., 2016). However, the mechanisms of the two states are distinct. Adsorbed hydrocarbons interact with the surface of kerogen through Van der Waals and Coulomb forces (Curtis, 2002), while swelling hydrocarbons are shale oil that is "embedded" in the kerogen structure through swelling, which is a hydrocarbon compound surrounded by kerogen molecules in a solid solution state (van Heek, 2000; Li et al., 2016). To assess the quantitative amount of swelling hydrocarbons in the kerogen structure (excluding adsorption), a model was developed in this study to preliminarily evaluate the swelling of different hydrocarbon compounds.

The same kerogen sample was used for the swelling experiments in this study, allowing for the average particle size and composition to be considered consistent. As a result, the surface area of the sample (S) is only relevant to maturity. The mass of adsorbed hydrocarbons is influenced by the volume and density,

while the adsorption volume is determined by the adsorption area S. The k_S value can be employed to represent the relative volume change, with k being the assumed proportionality constant. Given these factors, the mass of hydrocarbons in the swollen state (M) within the kerogen structure can be evaluated as:

$$M = a - \rho k_{\rm S} \tag{1}$$

And the amount of swollen state hydrocarbon can be calculated by:

$$M_1 - M_2 = (a_1 - a_2) + (\rho_1 - \rho_2) k_S$$
 (2)

where M_1 and M_2 represent the amount of swollen state of the two hydrocarbons at the same maturity, and when M_1-M_2 is positive, it indicates that the swelling capacity of reagent 1 is greater than that of reagent 2; a_1 and a_2 represent the amount of hydrocarbon compounds swelling adsorption per gram of kerogen according to the swelling experiment; ρ_1 and ρ_2 represent the densities of the two reagents. Since k_S is a constant positive value, the sign of M_1-M_2 depends on the result of (a_1-a_2) and $(\rho_1-\rho_2)$. When both values are positive, the content of hydrocarbons in the swollen state of the 1 reagent must be greater than that of the 1 reagent.

Fig. 7 illustrates the density and swelling adsorption of various liquid hydrocarbons, allowing for a comparison of the relative content of each solvent's swollen state (the density of nine solvent is shown in Table 5). Alkanes, for instance, exhibit a direct correlation between the number of carbon atoms and the amount of swollen state. However, cyclopentane, despite having a higher density than n-undecane, has a lower swelling adsorption weight. This suggests that the interaction parameter a_1 - a_2 is negative, and

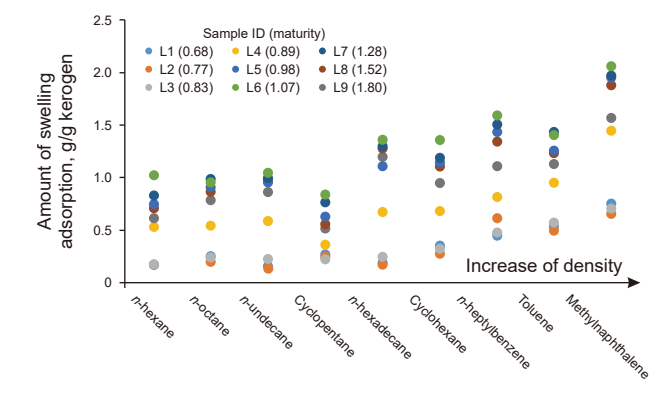


Fig. 7. Quantitative evaluation model for swollen state hydrocarbon compound.

Table 5 Density of solvent.

Solvent	Density, g/cm ³
n-hexane	0.66
n-octane	0.703
n-undecane	0.74
Cyclopentane	0.751
n-hexadecane	0.7734
Cyclohexane	0.791
n-heptylbenzene	0.861
Toluene	0.872
Methylnaphthalene	1.025

cyclopentane's swelling capacity is likely lower than that of nundecane. A similar trend is observed in the comparisons of cyclohexane—*n*-hexadecane and toluene—*n*-heptylbenzene groups. This indicates that kerogen has limited ability to swell cyclic compounds, whether cycloalkanes or monocyclic aromatics. It is possible that more of these compounds' retained hydrocarbons are in the adsorbed state. Nevertheless, long-chain alkanes and polycyclic aromatic hydrocarbons are more likely to form a solid solution state (swelling state) within the molecular structure of kerogen. Consequently, in this study, n-hexadecane and methylnaphthalene exhibit the strongest swelling ability in kerogen. Therefore, it is plausible that longer alkanes and compounds with more aromatic rings are more likely to remain in solid solution within kerogen. Long-chain alkanes and polycyclic aromatic hydrocarbons are preserved in the structure of solid organic matter in the form of swelling and adsorption, and it is more difficult to expel hydrocarbons than other small-molecule compounds. In particular, compounds in the swollen state may play an important role in secondary cleavage.

4. Conclusion

The ability of type I kerogen to retain aromatic compounds is stronger than that of saturated hydrocarbons, and with the increasing of maturity, alkanes show a trend of decreasing, while aromatics increase. The ability of liquid hydrocarbons to swell and adsorb reaches its peak at Easy% $R_0 = 1.07$. The order of hydrocarbon expulsion from source rocks is: short-chain alkanes > cycloalkanes/long-chain alkanes > aromatics with alkyl groups > polycyclic aromatic hydrocarbons. As a result, short-chain alkanes, cycloalkanes, and benzene series are more likely to complete hydrocarbon expulsion firstly.

The swelling state evaluation model indicates that long-chain alkanes and polycyclic aromatic hydrocarbons have the highest potential for swelling state occurrence in type I kerogen. Therefore, paraffin and asphaltenes based on these two compounds are more likely to be stable in the kerogen and less likely to be quickly excluded. In the exploration and exploitation of conventional oil, shale oil and heavy oil, paraffin and asphaltene may be the focus of research, particularly in immature source rocks.

CRediT authorship contribution statement

Tian Liang: Writing – original draft, Funding acquisition, Data curation. **Yan-Rong Zou:** Writing – review & editing. **Zha-Wen Zhan:** Writing – review & editing. **Ping-An Peng:** Writing – review & editing.

Declaration of competing interest

The authors declare that they have no known competing financial interests or personal relationships that could have appeared to influence the work reported in this paper.

Acknowledgements

This work was financially supported by Guangdong Basic and Applied Basic Research Foundation (2023A1515011646). This work was financially supported by the Director's Fund of Guangzhou Institute of Geochemistry, CAS (2022SZJ5T-06) and Open Fund of SINOPEC Petroleum Exploration and Production Research Institute. Thanks for the Petroleum Science editor and reviewers for their comments on this research. This is contribution No.IS-3682 from GIGCAS.

References

- Ballice, L., 2003. Solvent swelling studies of Göynük (Kerogen Type-I) and Bey-pazarı oil shales (Kerogen Type-II). Fuel 82 (11), 1317–1321. https://doi.org/10.1016/S0016-2361(03)00026-7.
- Behar, F., Roy, S., Jarvie, D., 2010. Artificial maturation of a Type I kerogen in closed system: Mass balance and kinetic modelling. Org. Geochem. 41 (11), 1235–1247. https://doi.org/10.1016/j.orggeochem.2010.08.005.
- Berger, I.A., 1960. Diagenesis of metabolites and a discussion of the origin of petroleum hydrocarbons. Geochem. Cosmochim. Acta 19 (4), 297–308. https://doi.org/10.1016/0016-7037(60)90036-3.
- Berlendis, S., Beyssac, O., Derenne, S., et al., 2014. Comparative mineralogy, organic geochemistry and microbial diversity of the Autun Black shale and Graissessac coal (France). Int. J. Coal Geol. 132, 147–157. https://doi.org/10.1016/j. coal.2014.07.005.
- Cao, H.R., Lei, Y., Wang, X.Y., et al., 2021. Molecular structure evolution of Type I kerogen during pyrolysis: Case study from the Songliao Basin, NE China. Mar. Petrol. Geol. 134, 105338. https://doi.org/10.1016/j.marpetgeo.2021.105338.
- Curtis, J.B., 2002. Fractured shale-gas systems. AAPG Bull. 86 (11), 1921–1938. https://doi.org/10.1306/61EEDDBE-173E-11D7-8645000102C1865D.
- Durand, B., Monin, J.C., 1980. Elemental analysis of kerogens. In: Durand, B. (Ed.), Kerogen, Insoluble Organic Matter from Sedimentary Rocks. Editions Technip, Paris, pp. 113–142.
- Fester, J.I., Robinson, W.E., 1966. Oxygen functional groups in Green River oil-shale kerogen and trona acids. In: Gould, R.F. (Ed.), Coal Science. American Chemical Society, Wash-ington, DC, pp. 22–31.
- GB/T19144-2010. Isolation Method for Kerogen from Sedimentary Rock (in Chinese).
- Gao, Y., Zou, Y.Y., Peng, P.A, 2017. Jump in the structure of Type I kerogen revealed from pyrolysis and ¹³C DP MAS NMR. Org. Geochem. 112, 105–118. https://doi. org/10.1016/j.orggeochem.2017.07.004.
- He, K., Zhang, S.C., Mi, J.K., et al., 2018. The evolution of chemical groups and isotopic fractionation at different maturation stages during lignite pyrolysis. Fuel 211, 492–506. https://doi.org/10.1016/j.fuel.2017.09.085.
- He, K., Zhang, S.C., Mi, J.K., et al., 2019. Carbon and hydrogen isotope fractionation for methane from non-isothermal pyrolysis of oil in anhydrous and hydrothermal conditions. Energy Explor. Exploit 37, 1558–1576. https://doi.org/ 10.1177/0144598719857189.
- Hu, T., Pang, X.Q., Jiang, F.J., et al., 2021. Movable oil content evaluation of lacustrine organic-rich shales, methods and a novel quantitative evaluation model. Earth Sci. Rev. 214, 103545. https://doi.org/10.1016/j.earscirev.2021.103545.
- Huang, L., Khoshnood, A., Firoozabadi, A., 2020. Effect of swelling by organic solvent on structure, pyrolysis, and methanol extraction performance of Hefeng Bituminous Coal. Energy Fuel 267, 117155. https://doi.org/10.1021/acsomega.0c06105.
- Hunt, J.M., 1972. Distribution of carbon in crust of Earth. AAPG 56 (11), 2273–2277. https://doi.org/10.1306/819A4206-16C5-11D7-8645000102C1865D.
- Jarvie, D.M., 2012. Shale resource systems for oil and gas: Part 2: Shale-oil resource systems. Shale reservoirs-giant resources for the 21st century. AAPG Mem 97, 89–119. https://doi.org/10.1306/13321447M973489.
- Kelemen, S.R., Walters, C.C., Ertas, D., et al., 2006. Petroleum expulsion part 2. Organic matter type and maturity effects on kerogen swelling by solvents and thermodynamic parameters for kerogen from regular solution theory. Energy Fuel 20 (1), 301–308. https://doi.org/10.1021/ef0580220.
- Kilk, K., Savest, N., Yanchilin, A., et al., 2010. Solvent swelling of Dictyonema oil shale: Low temperature heat-treatment caused changes in swelling extent.
 J. Anal. Appl. Pyrolysis 89 (2), 261–264. https://doi.org/10.1016/j.iaap.2010.09.003.
- Klemme, H., Ulmishek, G.F., 1991. Effective petroleum source rocks of the world: Stratigraphic distribution and controlling depositional factors. AAPG Bull. 75 (12), 1809–1851. https://doi.org/10.1306/BDFF8A7E-1718-11D7-8645000102C1865D.
- Larter, S.R., Huang, H.P., Snowdon, L., et al., 2012. What we do not know about self-sourced oil reservoirs: Challenges and potential solutions. In: SPE 162777, pp. 1-4.
- Lewan, M.D., Roy, S., 2011. Role of water in hydrocarbon generation from Type-I kerogen in Mahogany oil shale of the Green River Formation. Org. Geochem. 42 (1), 31–41. https://doi.org/10.1016/j.orggeochem.2010.10.004.
- Li, Z., Zou, Y.R., Xu, X.Y., et al., 2016. Adsorption of mudstone source rock for shale oil-experiments, model and a case study. Org. Geochem. 92, 55–62. https://doi.org/10.1016/j.orggeochem.2015.12.009.

- Liang, T., Zhu, F., Zhan, Z.W., et al., 2025. Study on hydrocarbon retention and expulsion of kerogen based on centrifugal swelling method. Org. Geochem. 201, 104921. https://doi.org/10.1016/j.orggeochem.2024.104921.
- Liang, T., Zou, Y.R., Zhan, Z.W., et al., 2021. Chemical structure changes of solid bitumen during solvent swelling investigated by X-ray diffraction. Int. J. Coal Geol. 243, 103778. https://doi.org/10.1016/j.coal.2021.103778.
- Liang, T., Zhan, Z.W., Zou, Y.R., et al., 2023. Research on type I kerogen molecular simulation and docking between kerogen and saturated hydrocarbon molecule during oil generation. Chem. Geol. 617, 121263. https://doi.org/10.1016/j. chemgeo.2022.121263.
- Liang, T., Zou, Y.R., Zhan, Z.W., Lin, X.H., Shi, J., Peng, P., 2020. An evaluation of kerogen molecular structures during artificial maturation. Fuel 265, 116979. https://doi.org/10.1016/j.fuel.2019.116979.
- Mao, J.D., Fang, X.W., Lan, Y.Q., et al., 2010. Chemical and nanometer-scale structure of kerogen and its change during thermal maturation investigated by advanced solid-state ¹³C NMR spectroscopy. Geochem. Cosmochim. Acta 74 (7), 2110–2127. https://doi.org/10.1016/j.gca.2009.12.029.Romero-Sarmientoa, M.F., Rohaisa, S., Littke, R., 2019. Lacustrine Type I kerogen
- Romero-Sarmientoa, M.F., Rohaisa, S., Littke, R., 2019. Lacustrine Type I kerogen characterization at different thermal maturity levels: Application to the Late Cretaceous Yacoraite Formation in the Salta Basin-Argentina. Int. J. Coal Geol. 203, 15–27. https://doi.org/10.1016/j.coal.2019.01.004.

- Sandvik, E.I., Young, W.A., Curry, D.J., 1992. Expulsion from hydrocarbon sources: The role of organic absorption. Org. Geochem. 19 (1–3), 77–87. https://doi.org/10.1016/0146-6380(92)90028-V.
- Sweeney, J.J., Burnham, A.K., 1990. Evaluation of a simple model of vitrinit reflectance based on chemical kinetics. AAPG Bull. 74 (10), 1559–1570. https://doi.org/10.1306/0C9B251F-1710-11D7-8645000102C1865D.
- Tissot, B., Deroo, G., Hood, A., 1978. Geochemical study of the Uinta Basin: Formation of petroleum from the Green River Formation. Geochem. Cosmochim. Acta 42 (10), 1469–1485. https://doi.org/10.1016/0016-7037(78)90018-2.
- van Heek, K.H., 2000. Progress of coal science in the 20th century. Fuel 79 (1), 1–26. https://doi.org/10.1016/S0016-2361(99)00190-8.
- Vandenbroucke, M., Largeau, C., 2007. Kerogen origin, evolution and structure. Org. Geochem. 38 (5), 719–833. https://doi.org/10.1016/j.orggeochem.2007.01.001.
- Wei, Z.F., Zou, Y.R., Cai, Y.L., et al., 2012. Kinetics of oil group-type generation and expulsion, an integrated applicationto Dongying Depression, Bohai Bay Basin, China. Org. Geochem. 52, 1–12. https://doi.org/10.1016/j.orggeochem.2012.08.006.
- Zhang, Z.R., Volkman, J.K., 2020. Isotopically enriched n-alkan-2-ones with even chain predominance in a torbanite from the Sydney Basin, Australia. Org. Geochem. 144, 104018. https://doi.org/10.1016/j.orggeochem.2020.104018.